Available online at www.sciencedirect.com

ScienceDirect

Rice Science, 2023, 30(6): 587−597

Research Paper

Seed-Specific Expression of Apolipoprotein A-I$_{Milano}$ Dimer in Engineered Rice Lines

Serena REGGI[1], Elisabetta ONELLI[2], Alessandra MOSCATELLI[2], Nadia STROPPA[2], Matteo DELL'ANNO[1], Kiril PERFANOV[3], Luciana ROSSI[1]

([1]*Department of Veterinary Medicine and Animal Science, University of Milan, Lodi 26900, Italy;* [2]*Department of Biosciences, University of Milan, Milan 20133, Italy;* [3]*Plantechno Srl, Casalmaggiore 26040, Italy*)

Abstract: Apolipoprotein A-I$_{Milano}$ (ApoA-I$_M$) has been shown to significantly reduce coronary atherosclerotic plaques. However, the preparation of cost-effective pharmaceutical formulations of ApoA-I$_M$ is limited by the high cost and difficulty of purifying the protein and producing the highly effective dimeric form. The aim of this study was to create an expression cassette that specifically drives the expression of dimeric ApoA-I$_M$ in the protein bodies of rice seeds. The ApoA-I$_M$ protein under control of the 13 kDa prolamin promoter is expressed exclusively in its dimeric form within the seeds, and immunocytochemical and immunogold analyses confirmed its expression in different caryopsis tissue such as seed coat, aleurone cell and endosperm, particularly in amyloplast and storage vacuoles. A plant-based ApoA-I$_M$ production system offered numerous advantages over current production systems, including the direct production of the most therapeutically effective dimeric ApoA-I$_M$ forms, long-term protein storage in seeds, and ease of protein production by simply growing plants. Therefore, seeds had the potential to serve as a cost-effective source of therapeutic ApoA-I$_M$.

Key words: apolipoprotein A-I$_{Milano}$; engineered plant; immunofluorescence; immunogold analysis; rice; seed-specific promoter

Apolipoprotein A-I (ApoA-I) is a component of high-density lipoprotein (HDL). It constitutes approximately 65%–70% of the protein mass in HDL. HDL is a molecule that transports cholesterols and phospholipids through the bloodstream from body tissues to livers, where they can be metabolized or removed from the body (Ben-Aicha et al, 2020). HDL is often called 'good cholesterol' due to its ability to reduce the risk of heart and cardiovascular diseases (Tardif et al, 2007). ApoA-I is the subject of intense research for its anti-atherogenic properties. The infusion of ApoA-I mimetic peptides stimulates cholesterol efflux from tissues into the bloodstream (Smith, 2010).

The naturally occurring variant ApoA-I$_{Milano}$ (ApoA-I$_M$) contains a cysteine residue at position 173 (R173C) that promotes disulphide bonds and the subsequent formation of dimers. Dimers increase protein stability (Alexander et al, 2009) and promote a greater interaction with lipids and enzyme lecithin-cholesterol acyltransferase, thereby increasing the therapeutic effect of the protein (Chiesa and Sirtori, 2003). ApoA-I$_M$ dimers can form HDL particles with the same efficiency as ApoA-I (Petrlova et al, 2014). Chyu and Shah (2015) indicated that 'HDL Therapy' with infusions of a formulation (ETC-216: Synthetic HDL phospholipids complex) of ApoA-I$_M$ significantly reduces coronary atherosclerotic plaques.

Although the therapeutic effects of apolipoproteins have been proven, there are numerous difficulties in their pharmaceutical preparation, mainly related to the

Received: 21 January 2023; **Accepted:** 19 June 2023
Corresponding author: Alessandra MOSCATELLI (alessandra.moscatelli@unimi.it)

Peer review under responsibility of China National Rice Research Institute
http://dx.doi.org/10.1016/j.rsci.2023.09.001

high cost of production. The production of recombinant proteins in bacterial systems is attractive for their capacity to produce high quantities but also faces difficulties such as the presence of undesirable affinity signals at the end of the purification progress (Rosano and Ceccarelli, 2014). Furthermore, the endotoxins of *Escherichia. coli* are known to form strong complexes with apolipoproteins (Emancipator et al, 1992). The elimination of these toxins for pharmaceutical products is necessary and technically possible but requires complex and costly methods (Mamat et al, 2015). Producing the more therapeutically effective dimeric form of ApoA-I_M can be accomplished by purifying monomers from *E. coli*, as described in patent US6617134B1, with a subsequent dimerization process. However, this is a time-consuming and expensive procedure that is not without risks.

To overcome these challenges, there is a need for an expression system that can easily, safely, and cost-efficiently produce apolipoproteins in their dimeric form. The ability to introduce foreign genes into plant species through techniques such as agro-infection or direct gene transfer has opened up the possibility of using engineered plants as host organisms for the production of heterologous proteins (Schmidt et al, 1997; Streatfield, 2007). Plants offer several advantages for this purpose: i) they represent an economical system, compared with mammalian cell cultures and microbial fermentation; ii) the expression of heterologous proteins can be induced in specific organs such as seeds, and tubers, where proteins are more stable (Torres et al, 2001; Onelli et al, 2017); iii) therapeutic proteins derived from plants, whether purified or not, are less likely to be contaminated with human pathogenic microorganisms than those derived from animal cells because plants are not hosts for human or animal infectious agents (Rossi et al, 2014b; Oluwayelu and Adebiyi, 2016); iv) plants can perform most of the post-translational modifications (eg., glycosylation and prenylation) required for protein stability and bioactivity in the same way as other higher eukaryotes; and v) proteins can be expressed in the edible organs of plants to be consumed raw as edible vaccines, eliminating the need for downstream processes (Rossi et al, 2014a; Gunasekaran and Gothandam, 2020). When downstream processing is required, it is simpler and less expensive, especially when proteins are expressed in specific organs like seeds.

A previous study demonstrated that rice plants transformed for ApoA-I_M expression produce rice milk with valuable therapeutic effects, protecting mice from atherosclerotic plaques and suggesting the potential use of these molecules in cardiovascular diseases (Romano et al, 2018). Rice seeds are an ideal platform for molecular farming due to their high grain yield, genetic purity maintained through self-pollination, ease of transformation, and suitability for oral delivery. Rice endosperm contains starch particles and proteins: 60%–80% of storage proteins are glutelins, and 20%–40% are prolamins. Protein bodies (PBs) such as PB-I and PB-II, in rice seeds are specialized storage organs for protein in seeds. Recombinant proteins bioencapsulated in PBs demonstrate higher resistance to digestion than proteins located in other intracellular compartments and remain highly stable for one year at room temperature. The administration of recombinant proteins expressed in rice seeds is safe and economically attractive as oral drugs or minimally processed functional nutrients (Takaiwa et al, 2017; Zhu et al, 2022).

The aim of this study was to evaluate an expression cassette driving the specific expression of dimeric ApoA-I_M within the PBs of rice seeds. In addition, ApoA-I_M transformed rice plants were characterized, and the localization of the protein was investigated at different stages of seed ripening in these engineered plants.

RESULTS

Expression vector and molecular analysis of putative transformed plants

An expression vector for rice, designated pCAMBIA-PROL-ApoA-I_M (Fig. S1-A), was developed to carry the ApoA-I_M gene under the control of the putative 13 kDa prolamin promoter. In order to confirm the correct insertion of the ApoA-I_M gene and the promoter into the expression vector pCAMBIA-PROL-ApoA-I_M, the plasmid was digested with different restriction enzymes and subjected to electrophoresis on agarose gels. The sizes of the digested fragments matched the expected size according to the map of recombinant plasmid (Fig. S1-B). The fusion of the promoter and gene, as well as the correct reading frame for translation, were confirmed by Sanger sequencing. A total of 100 calli derived from mature embryos of the rice variety Rosa Marchetti were transformed by agro-infection, and approximately 32 independent hygromycin-resistant T_0 transformed plants were obtained and then grown under the greenhouse conditions for evaluating morphology and fertility. Considering the seeds production, about 93% of the transformed plants were

fertile and displayed morphological characteristics similar to the controls (untransformed plants).

PCR analysis was conducted on all independently derived engineered plants to ascertain the presence of the ApoA-I_M gene using specific primers (Apo-fw and Apo-rv, Table S1). Plants harboring the ApoA-I_M gene yielded a band of the expected size, corresponding to PCR product of 732 bp (Fig. S1-C). No amplification was detected in the genome of wild type seeds (negative control). Approximately 72% of the rice plants were confirmed as transformed. The absence of detectable PCR products in some plants, despite undergoing hygromycin selection, could be attributed to factors such as the development of antibiotic resistance, genetic instability after post-integration, and partial integration of the expression vector (Gelvin, 2003).

The status of the engineered plants was characterized in detail by Southern blot, and the number of transgene integration sites into the genome of engineered plants was estimated. We analyzed 16 independently derived T_0 engineered plants by Southern blot. Unique and complex hybridization patterns were revealed, indicating that these plants indeed originated from independent events (Fig. S2). All 16 engineered plants showed positive hybridization, with most hybridization bands between 3 kb and 8 kb. The majority of engineered plants carried multiple copies of the transgenes ApoA-I_M, while only four plants carried a single copy of the engineered gene (Fig. S2). No hybridization bands were found in the untransformed rice plants (used as controls). After transplanting to greenhouse, all T_0 engineered rice plants grew well and produced normal seeds similar to untransformed rice plants. Segregation for hygromycin resistance was observed in all independently transformed rice lines. The results indicated that the segregating ratios in plant lines (3, 15, 23, and 25) followed the classic Mendelian inheritance pattern of 3:1 (resistant to sensitive) and co-segregated with hygromycin resistance, confirming a single insertion site, as shown by a single band (Fig. S2). T_1 plants (including both multi-copy and single-copy plants) germinated from F_1 seeds were analyzed by Southern blot, demonstrating the stable integration and inheritance of exotic genes.

Expression analysis of ApoA-I_M in engineered plants

Sodium dodecyl sulfate-polyacrylamide gel electrophoresis (SDS-PAGE) analysis in the absence or presence of a reducing agent (dithiothreitol or β-mercaptoethanol) was used to detect cys-cys linked covalently dimers as reported by Petrlova et al (2014). All proteins from F_1 seeds of PCR-positive lines were separated via SDS-PAGE in the presence and absence of the reducing agent (+/- β-mercaptoethanol) followed by Western blot with antibodies specific for human ApoA-I protein. Approximately 64% of the PCR-positive lines produced the monomeric ApoA-I_M, visualized as a specific band at variable levels of 28 kDa, corresponding to the molecular weight of the monomer ApoA-I (Fig. 1-A and -C). Results of gene expression showed different transcription levels of ApoA-I mRNA in engineered plants ($P \leq 0.05$; Fig. 1-B), confirming the different band intensities observed in Western Blot. At the same time, the F_1 seeds producing ApoA-I_M monomers were analyzed under non-reducing conditions, and 75% of the rice seeds exhibited a second band at about 56 kDa, corresponding to the molecular weight of the ApoA-I_M dimer, a feature not present in wild type rice seeds. The relative expression levels of monomeric and/or dimeric forms of the ApoA-I_M protein in seed extracts differed among the analyzed plant lines. The ApoA-I_M quantity was quantified by Enzyme-linked immunosorbent assay, and the expression level was resumed in Table S2. There was no cross reactivity between the ApoA-I polyclonal antibody and any endogenous proteins in untransformed rice seeds. ApoA-I_M accumulated in rice seeds in variable quantity, with the highest recovery reaching 82 mg/kg of rice seeds. The number of gene copies of the introduced ApoA-I_M genes could not be strictly correlated with the expression levels in the same plants, suggesting that the variation in expression resulted from other factors, such as chromosomal position effects of the integrated genes in the *Oryza* genome.

The glycosylation prediction study showed one possible site at position 16 (NASA) located in the signal peptide of the promoter (Fig. 1-D). Prediction studies of promoter cleavage confirmed a 99.3% possibility of cleavage occurring at the same position (16), generating a free signal peptide and a mature protein. In order to investigate the presence of different isoforms of ApoA-I due to post-translational modification, transformed seed proteins were separated by two-dimensional gel electrophoresis. This technique allowed the separation of polypeptides with a isoelectric point ranging from 3.6 to 9.3 and molecular masses from 14 to 120 kDa (Fig. S3). Western blot analysis (under reducing conditions) using anti-ApoA-I antiserum showed a faint reaction with a single spot, suggesting that the protein was not post-translationally modified.

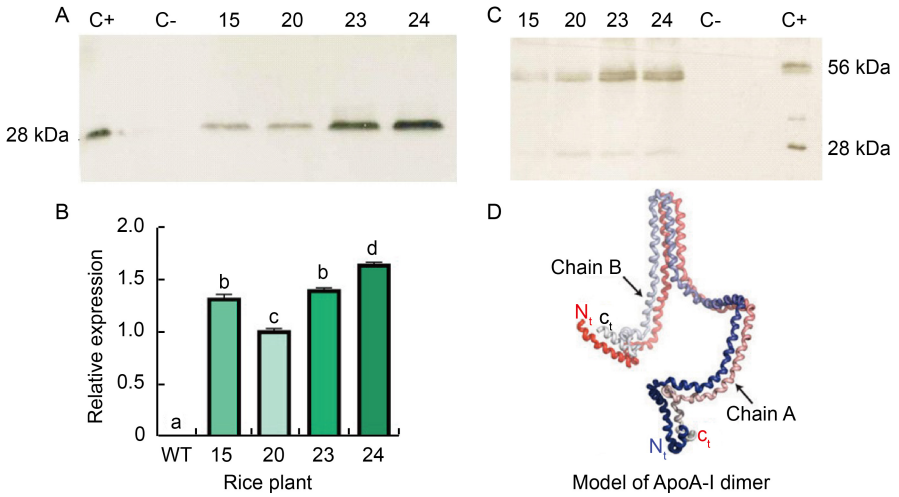

Primary structure:

MKIIFVFALLAIVACNASASRGSDEPPQSPWDRVKDLATVYVDVLKDSGRDYVSQFEGS
ALGKQLNLKLLDNWDSVTSTFSKLREQLGPVTQEFWDNLEKETEGLRQEMSKDLEEV
KAKVQPYLDDFQKKWQEEMELYRQKVEPLRAELQEGARQKLHELQEKLSPLGEEMR
DRARAHVDALRTHLAPYSDELRQCLAARLEALKENGGARLAEYHAKATEHLSTLSEKA
KPALEDLRQGLLPVLESFKVSFLSALEEYTKKLNTQSDI

Fig. 1. Western blot under reducing and non-reducing conditions, and the model of ApoA-I dimer by Gogonea et al (2013).

A, Western blot under reducing conditions (with β-mercaptoethanol); C+, ApoA-I recombinant; C-, Untransformed rice; ID 15, 20, 23, and 24 rice plants were positive in the screening PCR. All plants showed a band at 28 kDa, similar to the positive control, which was not present in the wild type (WT, untransformed rice) seeds.

B, Relative expression of ApoA-I_{Milano} gene in rice plants. RNA was extracted from rice seeds of different plants, and *beta-tubulin* was used as housekeeping gene. ID 15, 20, 23, and 24 rice plants were positive in the screening PCR. Results are presented as Mean ± SE from three biological replicates. Different lowercase letters above the bars indicate statistically significant differences at the level of $P \leq 0.05$.

C, Western blot under non-reducing conditions (without β-mercaptoethanol). ID 15, 20, 23, and 24 rice plants were positive in the screening PCR; C-, Untransformed rice; C+, Serum from patient Milano from the biological collection of 4LAB Diagnostics Srl.

D, Model of ApoA-I dimer reconstituted in dimyristoyl phosphatidyl choline by Gogonea et al (2013). Hypothetical three-dimensional model of ApoA-I dimer represented as a continuous helix. The two chains of ApoA-I were gradient coloured with red and blue, with the N termini coloured in red/blue and C termini coloured in light red/blue. Primary structure: the signal peptide of the prolamine promoter is listed in green and the predicted glycosylation site according to Gupta and Brunak (2002) is coloured in red. The ApoA-I_{Milano} mutation is highlighted in purple, corresponding to position 173 of the protein.

Temporal and spatial expression of ApoA-I_M protein

Prolamins are important storage proteins in rice, and they are classified by size as 10, 13, and 16 kDa (Muench et al, 1999). The temporal expression of the 13 kDa prolamin promoter was initially confirmed by differential display experiments conducted at different days after flowering (DAF) in rice seeds.

To investigate the role of the 13 kDa prolamin in the temporal expression of ApoA-I_M, 80 μg total proteins, isolated from engineered seeds at different ripening stages (4, 8, 12, 16, 20, and 25 DAF), were loaded onto a 15% acrylamide gel under denaturing conditions. After blotting onto a nitrocellulose membrane, hybridization with antiserum ApoA-I was performed. As shown in Fig. 2-A, the expression of the ApoA-I_M protein followed a time-course pattern during seed ripening. Western blot experiments revealed that the ApoA-I_M protein was detected at 12 DAF and rapidly accumulated to high levels during seed ripening. The level of expression remained stable until at complete seed maturation, consistent with Saito et al (2012). To confirm the expression pattern of the prolamin promoter during ripening stages, qRT-PCR was performed. As shown in Fig. 2-B, the ApoA-I_M transcript began at 12 DAF and peaked from 20 to 25 DAF until complete seed maturation.

Simultaneously, a Western blot analysis was performed on different rice tissues to verify seed-specific expression. Equal amounts (80 μg) of protein extracted from seeds, leaves, culms, and roots from ApoA-I_M engineered plants were blotted and hybridized under the same conditions. As shown in Fig. 2-C, the ApoA-I_M signal was only detected in the seeds, while leaves, culms, and roots showed an absence of positive hybridization, possibly due to prolonged exposure. RT-PCR confirmed that the 13 kDa prolamin promoter was active in directing ApoA-I_M expression only in the seeds (Fig. 2-D), indicating that the 13 kDa prolamin promoter in association with the NOS terminator is sufficient for

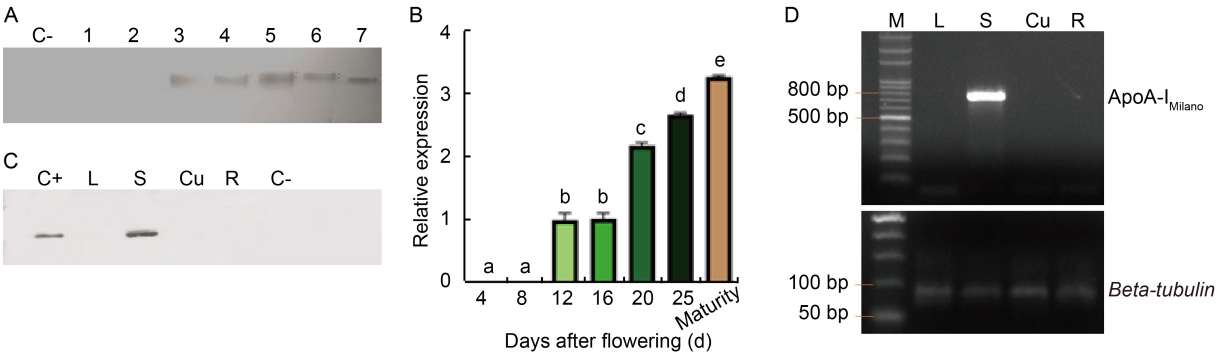

Fig. 2. Temporal and spatial expression of ApoA-I_M gene.

A, Western blot under reducing conditions (with β-mercaptoethanol). Rice seeds from the same panicle were collected at different days after flowering. Lines 1, 2, 3, 4, 5, 6, and 7 represent 4, 8, 12, 16, 20, and 25 days after flowering, and maturity stage, respectively.

B, qRT-PCR analysis of ApoA-I_M gene expression levels in seeds at different ripening stages. Results are presented as Mean ± SE from three biological replicates. Different lowercase letters above the bars indicate statistically significant differences at the level of $P \leq 0.05$.

C, Western blot under reducing conditions was performed on different plant tissues of the same transformed rice plant. The presence of the signal corresponding to positive control confirmed the seed-specificity of 13 kDa promoter.

D, RT-PCR carried out on different plant tissues. *Beta-tubulin* was used as the internal control.

C+, Recombinant hApoA-I; L, Proteins extracted from the leaf; S, Proteins extracted from transformed rice seeds; Cu, Proteins extracted from culm; R, Proteins extracted from roots; C-, Rice seeds from the untransformed plant.

seed specificity (Qu and Takaiwa, 2004).

Immunolocalization of ApoA-I_M in seed tissues

The localization of ApoA-I_M was further analyzed by immunocytochemical and immunogold observations. Within the same panicle we find caryopses at two developmental stages. These different caryopses (referred to as I and II) were collected from the same panicle (25 DAF) and characterized by fluorescence and electron microscopy.

In caryopsis I, the pericarp, seed coat and nucellus were clearly observed, with only weak autofluorescence observed in these tissues after anti-ApoA-I_M antibody treatment (Fig. 3-A and -B). In contrast, a high fluorescence was observed in the endosperm cells, while ApoA-I_M was excluded from aleurone cells. In the endosperm cells, ApoA-I_M was localized within amyloplasts (Fig. 3-C and -D), particularly in the stroma, surrounding starch granules which in turn appeared dark (Fig. 3-C and -D; indicated by arrows). Negative controls showed only faint autofluorescence and no cross-reaction with seed tissues (Fig. 3-E and -F).

The pattern of ApoA-I_M distribution changed in caryopsis II, in which the pericarp appeared thinner due to the flattening of mesocarp and seed coat cells (Fig. 3-G to -J). The nucellus also appeared compressed due to endosperm growth and was hardly recognizable (Fig. 3-H, -J, and -N). Immunofluorescence analysis showed that ApoA-I_M was localized not only in endosperm cells as in caryopsis I, but also in seed coat and aleurone cells (Fig. 3-G to -L), suggesting that during seed ripening, the expression and distribution of this protein changed. High fluorescence was observed in seed coat cells, while in pericarp cells, close to the seed coat, autofluorescence occurred as observed in the negative control (Fig. 3-I, -J, -K, and -L). In the endosperm, round organelles attributable to amyloplasts were fluorescent (Fig. 3-G to -J), and, interestingly, ApoA-I_M was also localized in both large and small organelles of the aleurone cells (Fig. 3-K and -L, indicated by arrows). Negative control always showed autofluorescence in pericarp cells (Fig. 3-M and -N).

To better investigate the ApoA-I_M localization inside cells, immunogold analysis was performed. Different anti-ApoAI$_M$ antibody concentrations were used to exclude nonspecific reactions with other cell components, and the observations confirmed the presence of ApoA-I_M predominantly in the endosperm, aleurone cells, and seed coat (Fig. 4). Interestingly, ApoA-I_M appeared to be preferentially localized in plastids. In the seed coat, ApoA-I_M was localized in chloroplasts (Fig. 4-A), particularly in the grana (Fig. 4-B). Aleurone cells were not fully differentiated, and some starch grains were also observed (Fig. 4-D). However, numerous storage vacuoles were stained with ApoA-I_M antibodies which were observed as dark spots (Fig. 4-D, arrows). In the endosperm, amyloplasts appeared bigger compared with those observed in aleurone cells and contained several starch granules (Fig. 4-E). ApoA-I_M was localized in both storage vacuoles and amyloplasts at the periphery of starch granules (Fig. 4-E; see arrows for amyloplast). Some

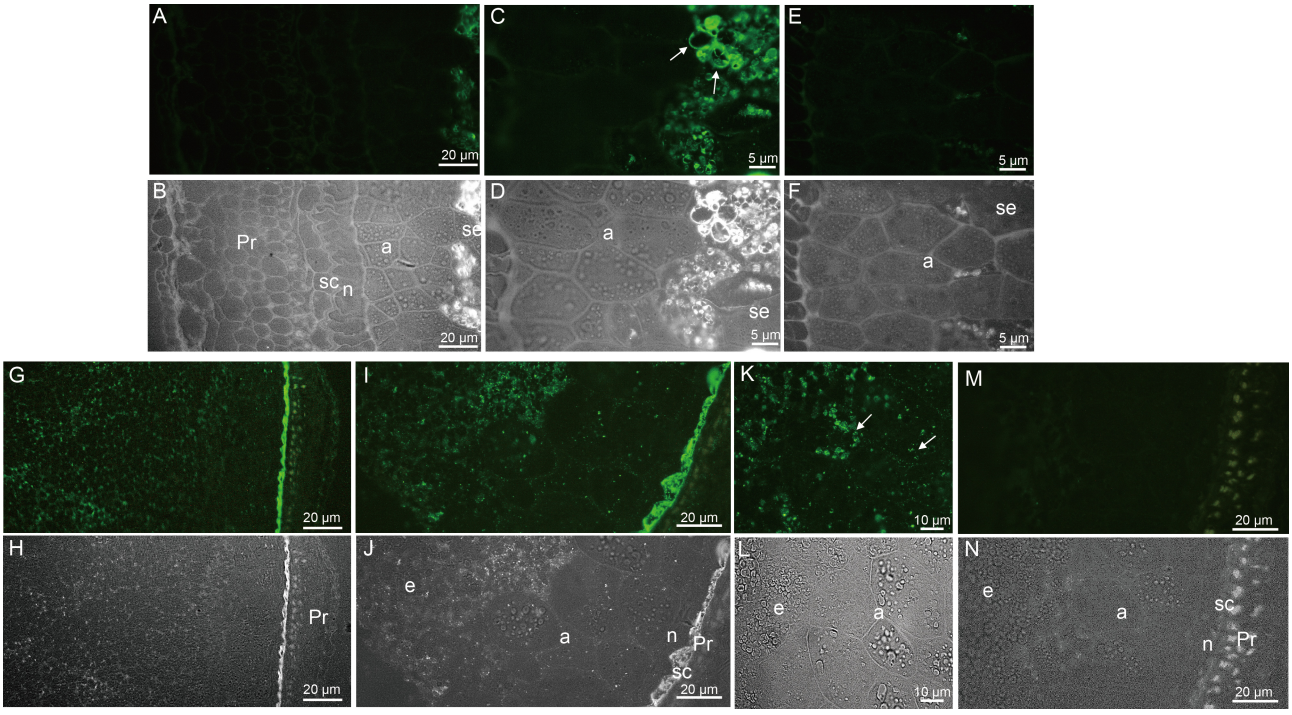

Fig. 3. Immunofluorescence and bright field images of caryopses I (A–F) and II (G–N) of ApoA-I_M transformed plants.

A–F, Immunofluorescence (**A**, **C**, and **E**) and bright field images (**B**, **D**, and **F**) of caryopsis I of ApoA-I_M transformed plant. For **A** and **C**, a high fluorescence was observed only in the amyloplasts of endosperm cells particularly in the stroma, surrounding starch granules in **C** with arrows. **E** and **F**, Negative controls showed no cross-reaction with seed tissues.

G–N, Immunofluorescence (**G**, **I**, **K**, and **M**) and bright field images (**H**, **J**, **L**, and **N**) of caryopsis II of ApoA-I_M transformed plant. Pericarp and nucellus appeared thinner in **G**, **H**, **I**, **J**, **M**, and **N**. ApoA-I_M was localized in organelles in endosperm cells, seed coats, and aleurone cells in **I** and **K** with arrows. **G** and **I**, High fluorescence was observed in the seed coat cells. **M** and **N**, Only autofluorescence was observed in negative control.

a, Aleurons cell; n, Nucellus; Pr, Pericarp; sc, Seed coat; se, Seed endosperm cell.

gold particles were also observed in the cell wall, particularly in the primary wall of seed coat and endosperm cells (Fig. 4-C and -F, arrows), as well as in Golgi-associated vesicles (Fig. 4-F, arrowheads). Negative control did not show any staining in plastids, vacuoles, or the cell wall (Fig. S4).

DISCUSSION

HDL and its major protein ApoA-I are protective against atherosclerosis through several mechanisms, including the ability to mediate reverse cholesterol transport. ApoA-I formulations and ApoA-I mimetic peptides have demonstrated rapid effects on plaque regression and stabilization (Smith, 2010). The natural variant Milano has been the subject of numerous studies and intriguing clinical trials (Nissen et al, 2003) that have highlighted its significant antiatherogenic properties (Sirtori et al, 2019). Recombinant expression of ApoA-I_M has been achieved in different systems (e.g. bacteria, yeasts, insect cells, and mammalian cells). Plants have been utilized for over two decades for the production of numerous pharmaceutical proteins, with promising results also in the realm of edible vaccines (Kurup and Thomas, 2020).

ApoA-I production in *E. coli* reported in the literatures ranges from 0.1 to 5.0 mg/L (Lorenzetti et al, 1986; Ryan et al, 2003), but in some cases, ApoA-I protein accumulates in inclusion bodies and requires refolding after purification. Nykiforuk et al (2011) expressed ApoA-I_M in a fusion protein in engineered safflower seeds at very high quantities, but ApoA-I_M rice offers certain advantages, including cost-effectiveness and large-scale production of readily usable edible materials.

Under the control of an RP5 prolamin promoter, ApoA-I_M was expressed in rice seeds at a maximum level of 49 mg/kg seeds, with its activity efficiently determined by Romano et al (2018). In this study, rice plants expressing ApoA-I_M under the control of a 13 kDa prolamin promoter were further investigated, particularly regarding seed expression and its cellular localization. The 13 kDa prolamin promoter (with its signal peptide) was demonstrated as an excellent candidate for ApoA-I_M expression in rice due to its seed-specificity and stability. The maximum recovery

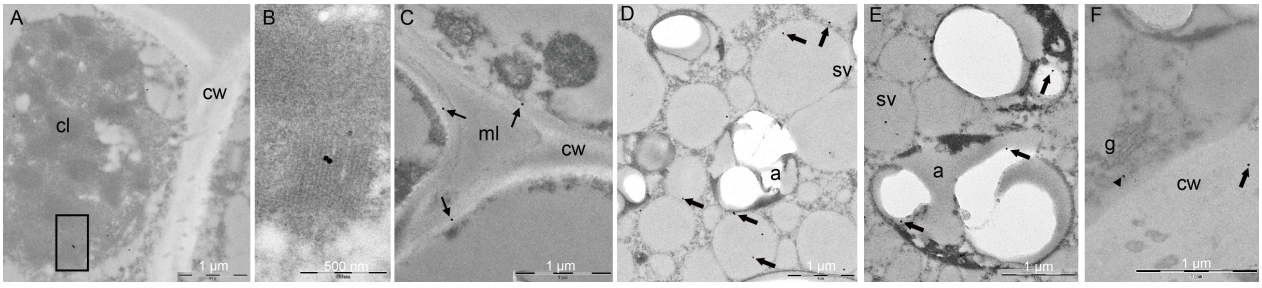

Fig. 4. Immunogold analysis on caryopsis II of ApoA-I$_M$ transformed plants.
A and **B**, ApoA-I$_M$ was localized into plasmids in the chloroplast grana in the seed coat (**B** is a magnification of box in **A**).
C, Dark spots were observed in the primary cell wall and not in middle lamellae (with arrows).
D, In aleuron cells, ApoA-I$_M$ was localized in storage vacuoles (with arrows).
E, ApoA-I$_M$ was localized into plasmids in amyloplasts of the endosperm cells (with arrows).
F, In aleuron cells, ApoA-I$_M$ was localized in vesicles associated with dictyiosomes (with arrowhead).
cl, Chloroplast; cw, Cell wall; ml, Middle lamellae; a, Amyloplast; sv, Storage vacuole; g, Golgi body.

of expression was 82 mg/kg of seeds, which is more efficient than the RP5 prolamin promoter. The promoter plays a fundamental role in determining spatial expression. The subcellular localization of a recombinant protein influences its stability, accumulation, and expression level. Protein targeting also plays a pivotal role in post‐translational modifications. Glycosylation is the most relevant modification in molecular farming because glycan chains affect protein structure, biological function, and immunogenicity. Targeting to a specific compartment cannot influence the correct folding, and the accumulation site has a direct impact on protein stability and protein recovery.

Both immunocytochemical (Fig. 3) and immunogold (Fig. 4) analyses showed that the recombinant protein ApoA-I$_M$ appeared to be localized in storage vacuoles. In rice endosperm, two different protein bodies were identified: PB-I characterized by the presence of prolamin while PB-II containes glutein and globulin (Tanaka et al, 1980; Saito et al, 2012). Since ApoA-I$_M$ is an exogenous animal protein under the control of the 13 kDa prolamin promoter, it is expressed in seed tissues as expected, but its localization within organelles appeared different compared with prolamin. In liver cells, ApoA-I$_M$ is synthesized in the endoplasmic reticulum lumen and then directed to the secretory pathway as a soluble protein (Stoffel, 1984). In plant cells, the expressed ApoA-I$_M$ protein does not possess a plant-specific signal for correct addressing in post-Golgi secretion. In the absence of specific receptors, soluble proteins may be collected in Golgi-derived secretory vesicles, as observed in Fig. 4, and randomly sorted towards vacuoles (presumably both PB-I and PB-II), the plasma membrane/cell wall and plastids (Kim and Brandizzi, 2014; Baslam et al, 2016). Interestingly, the presence of ApoA-I$_M$ in amyloplasts and chloroplasts suggests that a post-Golgi vesicle-mediated route is responsible for the delivery of proteins into plastids (Baslam et al, 2016). The mechanisms regulating vesicle transport to plastids are poorly understood. Three different hypotheses have been formulated: fusing/budding model, invagination model, and pass-through model (Baslam et al, 2016). As the ApoA-I$_M$ protein is sorted by a specific mechanism, it is not possible to ascribe it to one of these hypotheses. As observed in engineered tobacco seeds, obtained by the insertion of exogenous genes coding for seed-based oral vaccines (F18 and VT2eB), modified sorting of endogenous proteins can occur in transformed plants (Onelli et al, 2017). The sorting of ApoA-I$_M$ to different organelles appeared similar at two ripening stages. The obtained transformed plants offer a promising option for large-scale ApoA-I$_M$ production. Further investigations are required to better establish its effect after oral administration by edible transformed rice.

METHODS

Rice material and culture conditions

The seeds of *Oryza sativa* variety Rosa Marchetti were used for regeneration and transformation. They were surface-sterilized with a 5% sodium hypochlorite solution for 5 min, followed by 70% ethanol for 1 min, and washed 5 times with sterile distilled water. Embryo explants were cultured on 0.5× MS (Murashige and Skoog) solid medium. All cultures were maintained under controlled laboratory conditions at (28 ± 2) ºC under a 16 h light/8 h dark photoperiod with a cool white fluorescent lamp in a growth chamber. The ApoA-I$_M$ rice plants were cultivated in a biosafety greenhouse under ambient light conditions and the seeds were collected at the 4LAB Diagnostics Srl Laboratory

(Casalmaggiore, Italy).

Expression vector

The 13 kDa seed-specific promoter, along with its relative 5′-UTR (untranslated region) and transit peptide sequence (NCBI Acc. No. D63901 from -674 to +57), was amplified from *Oryza sativa* variety Ariete using forward and reverse primers (PROL-fw and PROL-rv, Table S1). The 729 bp promoter fragment was inserted into the pGEM-T vector (Promega, WI, USA), and the accuracy of the amplified promoter region was verified by DNA sequencing (Watts and MacBeath, 2001). *Pst* I and *Xba* I sites were respectively inserted in the forward and reverse primers to facilitate subsequent DNA cloning into a plant expression vector (pCAMBIA1302, NCBI Acc. No. AF234298) at *Pst* I and *Xba* I restriction enzyme cutting sites. The cDNA of mature ApoA-I_M, obtained from the biological collection at 4LAB Diagnostics Srl Laboratory (Casalmaggiore, Italy), was placed under the control of the rice 13 kDa prolamin promoter and cloned into the *Bam*H I and *Sac* I restriction enzyme cutting sites (blunted) (Fig. S1-A).

Rice transformation and analysis of engineered plants

Embryonic calli derived from mature zygotic embryos of Rosa Marchetti were inoculated with *Agrobacterium tumefaciens* strain EHA105 transformed by electroporation with the plasmid pCAMBIA-PROL-ApoA-I_M. Callus and bacterial induction, transformation, selection, and regeneration of engineered tissues were performed as described by Hiei et al (1994) with minor modifications. A number of independently transformed (hygromycin-resistant) plants (T_0 plants) were potted in peat and hardened in a greenhouse together with WT and self-pollinated to produce F_1 seeds. These F_1 seeds were then subsequently planted to produce T_1 plants (n = 3–5 of each line) and obtained F_2 seeds. During the entire experimental period, the plants were evaluated for the principal agronomic characteristics.

PCR analysis

Before flowering, T_0 and T_1 selected plants were subjected to PCR analysis to verify the presence of the transgene. DNA was extracted from leaves of the hygromycin-resistant rice lines, using the method described by Doyle and Doyle (1987). The primers Apo-fw and Apo-rv (Table S1) were used for PCR, amplifying the entire ApoA-I gene. Successful transformation would result in the visualization of a 732 bp fragment.

Southern blot analysis

Independent engineered rice plants from the T_0 and T_1 generations, positive in PCR, were subjected to Southern blot analysis to verify the number of transgene integration sites in each plant. Genomic DNA was extracted from young leaves according to Doyle and Doyle (1987). Approximately 10 μg of DNA was digested with *Xba* I which cuts only once in pCAMBIA-PROL-ApoA-I_M, and then separated on a 0.8% agarose gel. It was subsequently transferred to a positively charged nylon membrane, and hybridized with a probe corresponding to the ApoA-I_M coding sequences, labelled with the PCR DIG Probe Synthesis Kit (Roche Molecular Biochemicals, Penzberg, Germany) as per the manufacture's instructions. The primer set used in PCR analysis was also used to generate the DIG-labeled probe. The positive control included the vector (pGEMT-APOA-I_M) linearized with the same restriction enzyme. Detection was carried out with CDP-Star® (GE Healthcare, IL, USA) following the manufacturer's instructions. Segregation was studied by Southern blot analysis in selected plants (numbers 2–5) of the T_1 generation (Fig. S2-A).

Evaluation of protein expression

Western blot analysis

Seeds from the F_1 and F_2 generations collected respectively from the T_0 and T_1 PCR-positive plants were used to verify protein expression by Western blot analysis. Briefly, total proteins from rice seeds (100 mg) were extracted using an extraction buffer [50 mmol/L Tris-HCl pH 8.0, 5 mmol/L ethylene diamine tetraacetic acid (EDTA), 200 mmol/L NaCl, 0.1% Triton X-100, 1 mmol/L phenylmethanesulfonyl fluoride (PMSF)] in a 1:10 ratio, mixed with SDS-loading buffer (with or without β-mercaptoethanol, to discriminate from monomer/dimer, respectively). After Bradford protein quantification, 80 μg total soluble proteins were subjected to electrophoretic separation on an acrylamide gel and transferred using electroblotting (a solution of 25 mmol/L Tris, 192 mmol/L glycine, 20% methanol, 30 V at 4 ºC overnight) onto a nitrocellulose membrane (Hybond ECL, GE Healthcare, IL, USA). The membrane with the bound protein was placed in a solution of PBS-T and 5% skim milk, agitated for 1 h, washed, and then exposed to the primary antibody Anti ApoA-I Goat 1:5 000 (Acris, CA, USA) and subsequently to the secondary antibody anti-goat peroxidase conjugate, at 1:12 000 (Sigma Aldrich, MO, USA). The membrane was washed several times and placed in a chemiluminescent detection solution, ECL (GE Healthcare, IL, USA). The same extraction protocol was performed for protein extraction from leaves, culms, and roots.

Two-dimensional (2D) electrophoresis

Two-dimensional gel electrophoresis was performed with 50 μg extracted seed proteins precipitated with cold ethanol (1:5) and incubated for 30 min on ice. The pellet was obtained by centrifugation at 4 ºC for 36 min at 15 000 × g in an ALC A21-C rotor. Ethanol was removed, and the pellet was resuspended with 200 μL of rehydration buffer [8 mol/L urea, 4% 3-[(3-cholamidopropyl)dimethylammonio]-1-propanesulfonate hydrate (CHAPS), 65 mmol/L dithioerythritol, 0.5% bromophenol blue] supplemented with 2% IPG Buffer pH 3–10 NL (Cytiva Sweden AB, Uppsala, Sweden). This mixture was loaded onto 7-cm non-linear pH 3–10 strips and passively rehydrated overnight at room temperature. Isoelectric focusing was performed with the Multifor II system (GE Healthcare, IL, USA) according to Moscatelli et al (2015) (200 V for 1 h, 2 000 V for 3 h, and 3 000 V for 3 h and 30 min). Focused strips were equilibrated in Buffer I (0.5 mol/L Tris-HCl, pH 6.8, 2% SDS, 6 mol/L urea,

30% glycerol, 2% DTE) for 12 min and then for another 5 min in Buffer II (composition the same as Buffer I, but with 2.5% iodoacetamide instead of DTE) at room temperature. SDS-PAGE was conducted on a 10% polyacrylamide gel (MiniVertical Electrophoresis System, GE Healthcare, PA, USA), as previously described (Laemmli, 1970), and the gel was silver-stained (Sinha et al, 2001). After 2D electrophoresis, polypeptides were transferred onto a PVDF membrane (Amersham^{TM} Hybond, GE Healthcare, PA, USA) and tested for ApoA-I following protocol previously described for Western blot experiments.

The sequence related to the fusion of the signal peptide of the prolamine promoter and the mature ApoA-I_M gene was analyzed by NetNGlyc 1.0 Server for determination possible glycosylation sites. The glycosylation site prediction analysis was performed on the primary structure according to Gupta and Brunak (2002) for estimating possible post-translational modifications of ApoA-I_M.

Protein quantification in rice seeds

An indirect competitive ELISA (IC-ELISA) was used to detect ApoA-I_M protein in F_1 rice seeds. In particular, recombinant hApoA-I (Sigma Aldrich St. Louis, MO, USA) was coated at a concentration of 600 ng/mL onto a micro-well plate overnight at 4 ºC. The plate was then washed three times with 0.01 mol/L phosphate buffered saline (PBS, pH 7, Sigma Aldrich, MO, USA) and blocked with 200 µL of 5% BSA for 2 h at 37 ºC. Subsequently, the plate was washed with 0.01 mol/L PBS containing 0.05% Tween 20 (PBS-T). 100 µL of goat polyclonal anti-ApoA-I antibody (Acris, CA, USA) diluted 1 : 6000 was mixed with serial dilution (1:1, 1:10 and 1:50) of rice seed protein extraction (100 µL). From each mixture, a total of 100 µL solution was added to each well coated, and the plate was incubated at 37 ºC for 1 h. After incubation, the plate was washed with PBS-T and then a 1:5000 diluted solution (100 µL) of anti-goat IgG-HRP antibody (Thermo Fisher Scientific, Waltham, MA, USA) was added to each well and incubated at 37 ºC for 1 h. After that, the plate was rewashed with PBS-T, and a 50 µL solution of TMB (3,3′,5,5′-tetramethylbenzidine) was added to each well followed by incubation at 37 ºC for 15 min. To stop the reaction, 150 µL of 0.4 mol/L hydrochloric acid (HCl) was added to each well, and then absorbance was measured at 450 nm using an ELISA plate reader (Bio-Rad, CA, USA). Each experiment was performed in triplicates, and a standard curve using recombinant hApoA-I (Sigma Aldrich, MO, USA) protein was constructed.

RNA extraction, cDNA synthesis, RT-PCR, and qRT-PCR

Total RNA was isolated from leaves, culms, roots and seeds at different ripening stages in ApoA-I_M plants for gene expression analysis. Briefly, frozen tissue was grinded with an equal volume of RNA extraction buffer (0.1 mol/L Tris-HCl with pH 8, 50 mmol/L NaCl, 1 mmol/L EDTA, 0.5% EDTA and a 1 : 1 mixture of chloroform and phenol). RNA was precipitated with a LiCl at a final concentration of 2 mol/L (Takaiwa et al, 1987). The integrity of RNA was confirmed by electrophoresis on a 1.2% formaldehyde agarose gel.

cDNA synthesis was performed by the iScript cDNA synthesis kit (Bio-Rad, CA, USA) using a mixture of random primers and oligo dT, along with 2 µg of total RNA. Subsequently, 2 µL of cDNA generated from RNA extraction from leaves, seeds, culms, and roots were amplified in a PCR reaction with Apo-fw and Apo-rv primers (Table S1), as well as β-TUB primer (Jain et al, 2018). β-TUB mRNA was amplified with 20 cycles, and ApoA-I_M cDNA was amplified with 30 cycles using the standard PCR program following the instruction of the manufacturer of RedTaq ReadyMix PCR (Sigma-Aldrich, MO, USA). The cDNA transcript from RNA at different ripening stages of ApoA-I_M seeds was used in a qRT-PCR. qRT-PCR was performed using SsoAdvanced Universal SYBR Green Supermix (Bio-Rad, CA, USA) following the manufacturer's instructions. The reaction was performed on the CFX OPUS system (Bio-Rad, CA, USA) with a setting block standard, and initial denaturation at 98 ºC for 2 min, followed by 40 cycles at 98 ºC for 10 min and annealing/extension at 60 ºC for 30 s. Apo forward and reverse primers were used. The expression level was calculated using the $2^{-\Delta\Delta CT}$ method (Livak and Schmittgen, 2001), with *beta-tubulin* as the housekeeping gene (Jain et al, 2018). The calibrator was selected as the sample with the highest CT (cycle threshold) value or the lowest gene expression for relative expression.

Immunolocalization

Rice seeds were collected, cut into small pieces, and fixed in a solution containing 50 mmol/L Hepes with pH 7.4, 2% formaldehyde, and 0.2% glutaraldehyde, overnight at 4 ºC. Samples were then repeatedly rinsed with 50 mmol/L Hepes with pH 7.4, dehydrated using increasing concentrations of ethanol, and embedded in LR Gold resin (Sigma Aldrich, MO, USA) at -20 ºC. Semi-fine sections (2 µm) and ultra-thin sections (80 nm) were obtained using an Ultracut E microtome (Reichert Jung, Buffalo, USA). Ultra-thin sections were collected on nickel grids (Agar Scientific, Stansted, the United Kingdom) for immunogold experiments.

Immunofluorescence analysis

Semi-fine sections were hydrated with TBS (Tris-buffered saline, 20 mmol/L Tris, 150 mmol/L NaCl with pH 7.6) for 5 min, blocked with 1% bovine serum albumin (BSA, Sigma Aldrich, MO, USA) in TBS for 1 h at room temperature, and then incubated with primary goat polyclonal anti-ApoA-I antibody (Acris, CA, USA) diluted 1:500 overnight at 4 ºC. After three rinses in TBS, sections were incubated with the FITC-conjugated antigoat secondary anti-body (Santa Cruz Biotechnology, TX, USA) at a 1:200 dilution in TBS at room temperature for 2 h, followed by rinsing three times with TBS, and finally mounting the section in Cityfluor (Citofluor AF1, a triethylenediamine 5% glycerol/PBS solution) (Agar-Scientific, London, UK). Negative controls were performed using only the secondary antibodies. Fluorescence observations were performed

with a Leica DMRB microscope (set filter BP450-490, RKP 410, long pass 515), and images were captured using a Leica MC170 HD camera (Leica, Wetzlar, Germny).

Immunogold analysis

Ultra-thin sections were hydrated with TBS for a few minutes, blocked with 1% BSA in TBS for 30 min at room temperature, and incubated with primary goat polyclonal anti-ApoA-I antibody (Acris, San Diego CA, USA) at different dilutions (ranging from 1:500 to 1:200) in TBS at room temperature for 2 h. After three rinses in TBS, the sections were incubated with a 20 nm gold-conjugated rabbit anti-goat secondary antibody (BBA International, NY, USA) diluted 1:100 at room temperature for 1 h, and then rinsed three times with TBS, and post-fixed with 1% glutaraldehyde for 15 min at room temperature. Subsequently, the sections were that stained with 3% uranyl acetate for 20 min in the dark, rinsed with distilled water, dried, and observed using an EFTEM LEO 912AB transmission electron microscope (Zeiss, Oberkochen, Germany) operating at 100 kV.

Statistical analysis

The results of qRT-PCR were analyzed using GrapPad Prism software (version 9.0, GraphPad Software, CA, USA). Gene expression data from different rice plant clones were evaluated with analysis of variance (ANOVA) for unpaired samples. To assess statistical differences among different ripening days, a repeated measure ANOVA was used. The normality of residuals was verified using the D'Agostino-Pearson (K^2) test. Multiple pairwise comparisons were evaluated with Tukey's honestly significant differences test. Means were considered statistically different for $P \leq 0.05$.

ACKNOWLEDGMENT

The authors want to thank 4LAB diagnostics, Casalmaggiore, Italy, for providing the greenhouse facilities.

SUPPLEMENTAL DATA

The following materials are available in the online version of this article at http://www.sciencedirect.com/journal/rice-science; http://www.ricescience.org.

Fig. S1. Expression vector and molecular analysis of putative transformed plants.

Fig. S2. Southern blot analysis of engineered rice plants.

Fig. S3. Two-dimensional gel electrophoresis (A) and Western blot of bidimensional gel (B) of 50 μg of rice polypeptides extracted from ApoA-I transformed seeds.

Fig. S4. Negative control of seed tissues did not show antibody staining.

Table S1. Oligonucleotides used in this study for amplification of the ApoA-I gene and the 13 kDa prolamin promoter.

Table S2. T_0 rice plants obtained from transformation, relative controls (PCR, Western blotting, and Sothern analysis), and ApoA-I_M quantification by indirect competitive enzyme-linked immunosorbent assay (ELISA).

REFERENCES

Alexander E T, Tanaka M, Kono M, Saito H, Rader D J, Phillips M C. 2009. Structural and functional consequences of the Milano mutation (R173C) in human apolipoprotein A-I. *J Lipid Res*, **50**(7): 1409–1419.

Baslam M, Oikawa K, Kitajima-Koga A, Kaneko K, Mitsui T. 2016. Golgi-to-plastid trafficking of proteins through secretory pathway: Insights into vesicle-mediated import toward the plastids. *Plant Signal Behav*, **11**(9): e1221558.

Ben-Aicha S, Badimon L, Vilahur G. 2020. Advances in HDL: Much more than lipid transporters. *Int J Mol Sci*, **21**(3): 732.

Chiesa G, Sirtori C R. 2003. Apolipoprotein A-I_{Milano}: Current perspectives. *Curr Opin Lipidol*, **14**(2): 159–163.

Chyu K Y, Shah P K. 2015. HDL/ApoA-1 infusion and ApoA-1 gene therapy in atherosclerosis. *Front Pharmacol*, **6**: 187.

Doyle J J, Doyle J L. 1987. A rapid DNA isolation procedure for small quantities of fresh leaf tissue. *Phytochem Bull*, **19**(1): 11–15.

Emancipator K, Csako G, Elin R J. 1992. *In vitro* inactivation of bacterial endotoxin by human lipoproteins and apolipoproteins. *Infect Immun*, **60**(2): 596–601.

Gelvin S B. 2003. *Agrobacterium*-mediated plant transformation: The biology behind the "gene-jockeying" tool. *Microbiol Mol Biol Rev*, **67**(1): 16–37.

Gogonea V, Gerstenecker G S, Wu Z P, Lee X, Topbas C, Wagner M A, Tallant T C, Smith J D, Callow P, Pipich V, Malet H, Schoehn G, DiDonato J A, Hazen S L. 2013. The low-resolution structure of nHDL reconstituted with DMPC with and without cholesterol reveals a mechanism for particle expansion. *J Lipid Res*, **54**(4): 966–983.

Gunasekaran B, Gothandam K M. 2020. A review on edible vaccines and their prospects. *Braz J Med Biol Res*, **53**(2): e8749.

Gupta R, Brunak S. 2002. Prediction of glycosylation across the human proteome and the correlation to protein function. *Pac Symp Biocomput*, **7**: 310–322.

Hiei Y, Ohta S, Komari T, Kumashiro T. 1994. Efficient transformation of rice (*Oryza sativa* L.) mediated by *Agrobacterium* and sequence analysis of the boundaries of the T-DNA. *Plant J*, **6**(2): 271–282.

Jain N, Vergish S, Khurana J P. 2018. Validation of house-keeping genes for normalization of gene expression data during diurnal/ circadian studies in rice by RT-qPCR. *Sci Rep*, **8**: 3203.

Kim S J, Brandizzi F. 2014. The plant secretory pathway: An essential factory for building the plant cell wall. *Plant Cell Physiol*, **55**(4): 687–693.

Kurup V M, Thomas J. 2020. Edible vaccines: Promises and challenges. *Mol Biotechnol*, **62**(2): 79–90.

Laemmli U K. 1970. Cleavage of structural proteins during the assembly of the head of bacteriophage T4. *Nature*, **227**: 680–685.

Livak K J, Schmittgen T D. 2001. Analysis of relative gene expression data using real-time quantitative PCR and the $2^{-\Delta\Delta CT}$ method. *Methods*, **25**(4): 402–408.

Lorenzetti R, Sidoli A, Palomba R, Monaco L, Martineau D, Lappi D A, Soria M. 1986. Expression of the human apolipoprotein AI gene fused to the *E. coli*gene for β-galactosidase. *FEBS Lett*,

194(2): 347–350.

Mamat U, Wilke K, Bramhill D, Schromm A B, Lindner B, Kohl T A, Corchero J L, Villaverde A, Schaffer L, Head S R, Souvignier C, Meredith T C, Woodard R W. 2015. Detoxifying *Escherichia coli* for endotoxin-free production of recombinant proteins. *Microb Cell Fact*, **14**: 57.

Moscatelli A, Gagliardi A, Maneta-Peyret L, Bini L, Stroppa N, Onelli E, Landi C, Scali M, Idilli A I, Moreau P. 2015. Characterisation of detergent-insoluble membranes in pollen tubes of *Nicotiana tabacum* (L.). *Biol Open*, **4**(3): 378–399.

Muench D G, Ogawa M, Okita T W. 1999. The prolamins of rice. *In*: Shewry P R, Casey R. Seed Proteins. Dordrecht, the Netherlands: Springer: 93–108.

Nissen S E, Tsunoda T, Tuzcu E M, Schoenhagen P, Cooper C J, Yasin M, Eaton G M, Lauer M A, Sheldon W S, Grines C L, Halpern S, Crowe T, Blankenship J C, Kerensky R. 2003. Effect of recombinant ApoA-I Milano on coronary atherosclerosis in patients with acute coronary syndromes: A randomized controlled trial. *JAMA*, **290**(17): 2292–2300.

Nykiforuk C L, Shen Y, Murray E W, Boothe J G, Busseuil D, Rhéaume E, Tardif J C, Reid A, Moloney M M. 2011. Expression and recovery of biologically active recombinant Apolipoprotein AI_{Milano} from transgenic safflower (*Carthamus tinctorius*) seeds. *Plant Biotechnol J*, **9**(2): 250–263.

Oluwayelu D O, Adebiyi A I. 2016. Plantibodies in human and animal health: A review. *Afr Health Sci*, **16**(2): 640–645.

Onelli E, Moscatelli A, Gagliardi A, Zaninelli M, Bini L, Baldi A, Caccianiga M, Reggi S, Rossi L. 2017. Retarded germination of *Nicotiana tabacum* seeds following insertion of exogenous DNA mimics the seed persistent behavior. *PLoS One*, **12**(12): e0187929.

Petrlova J, Dalla-Riva J, Mörgelin M, Lindahl M, Krupinska E, Stenkula K G, Voss J C, Lagerstedt J O. 2014. Secondary structure changes in ApoA-I Milano (R173C) are not accompanied by a decrease in protein stability or solubility. *PLoS One*, **9**(4): e96150.

Qu L Q, Takaiwa F. 2004. Evaluation of tissue specificity and expression strength of rice seed component gene promoters in transgenic rice. *Plant Biotechnol J*, **2**(2): 113–125.

Romano G, Reggi S, Kutryb-Zajac B, Facoetti A, Chisci E, Pettinato M, Giuffrè M R, Vecchio F, Leoni S, De Giorgi M, Avezza F, Cadamuro M, Crippa L, Leone B E, Lavitrano M, Rivolta I, Barisani D, Smolenski R T, Giovannoni R. 2018. APOA-1Milano muteins, orally delivered *via* genetically modified rice, show anti-atherogenic and anti-inflammatory properties *in vitro* and in $Apoe^{-/-}$ atherosclerotic mice. *Int J Cardiol*, **271**: 233–239.

Rosano G L, Ceccarelli E A. 2014. Recombinant protein expression in *Escherichia coli*: Advances and challenges. *Front Microbiol*, **5**: 172.

Rossi L, Dell'Orto V, Vagni S, Sala V, Reggi S, Baldi A. 2014a. Protective effect of oral administration of transgenic tobacco seeds against verocytotoxic *Escherichia coli* strain in piglets. *Vet Res Commun*, **38**(1): 39–49.

Rossi L, Pinotti L, Agazzi A, Dell'Orto V, Baldi A. 2014b. Plant bioreactors for the antigenic hook-associated flgK protein expression. *Ital J Animal Sci*, **13**(1): 2939.

Ryan R O, Forte T M, Oda M N. 2003. Optimized bacterial expression of human apolipoprotein A-I. *Protein Expr Purif*, **27**(1): 98–103.

Saito Y, Shigemitsu T, Yamasaki R, Sasou A, Goto F, Kishida K, Kuroda M, Tanaka K, Morita S, Satoh S, Masumura T. 2012. Formation mechanism of the internal structure of type I protein bodies in rice endosperm: Relationship between the localization of prolamin species and the expression of individual genes. *Plant J*, **70**(6): 1043–1055.

Schmidt H H J, Genschel J, Haas R, Büttner C, Manns M P. 1997. Expression and purification of recombinant human apolipoprotein A-I in Chinese Hamster ovary cells. *Protein Expr Purif*, **10**(2): 226–236.

Sinha P, Poland J, Schnölzer M, Rabilloud T. 2001. A new silver staining apparatus and procedure for matrix-assisted laser desorption/ionization-time of flight analysis of proteins after two-dimensional electrophoresis. *Proteomics*, **1**(7): 835–840.

Sirtori C R, Ruscica M, Calabresi L, Chiesa G, Giovannoni R, Badimon J J. 2019. HDL therapy today: From atherosclerosis, to stent compatibility to heart failure. *Ann Med*, **51**(7/8): 345–359.

Smith J D. 2010. Apolipoprotein AI and its mimetics for the treatment of atherosclerosis. *Curr Opin Invest Drugs*, **11**(9): 989–996.

Stoffel W. 1984. Synthesis, transport, and processing of apolipoproteins of high density lipoproteins. *J Lipid Res*, **25**(13): 1586–1592.

Streatfield S J. 2007. Approaches to achieve high-level heterologous protein production in plants. *Plant Biotechnol J*, **5**(1): 2–15.

Takaiwa F, Kikuchi S, Oono K. 1987. A rice glutelin gene family: A major type of glutelin mRNAs can be divided into two classes. *Mol Gen Genet*, **208**(1/2): 15–22.

Takaiwa F, Wakasa Y, Hayashi S, Kawakatsu T. 2017. An overview on the strategies to exploit rice endosperm as production platform for biopharmaceuticals. *Plant Sci*, **263**: 201–209.

Tanaka K, Sugimoto T, Ogawa M, Kasai Z. 1980. Isolation and characterization of two types of protein bodies in the rice endosperm. *Agric Biol Chem*, **44**(7): 1633–1639.

Tardif J C, Grégoire J, L'Allier P L, Ibrahim R, Lespérance J, Heinonen T M, Kouz S, Berry C, Basser R, Lavoie M A, Guertin M C, Rodés-Cabau J. 2007. Effects of reconstituted high-density lipoprotein infusions on coronary atherosclerosis: A randomized controlled trial. *JAMA*, **297**: 1675–1682.

Torres E, Gonzalez-Melendi P, Stöger E, Shaw P, Twyman R M, Nicholson L, Vaquero C, Fischer R, Christou P, Perrin Y. 2001. Native and artificial reticuloplasmins co-accumulate in distinct domains of the endoplasmic reticulum and in post-endoplasmic reticulum compartments. *Plant Physiol*, **127**(3): 1212–1223.

Watts D, MacBeath J R. 2001. Automated fluorescent DNA sequencing on the ABI PRISM 310 Genetic Analyzer. *Methods Mol Biol*, **167**: 153–170.

Zhu Q L, Tan J T, Liu Y G. 2022. Molecular farming using transgenic rice endosperm. *Trends Biotechnol*, **40**(10): 1248–1260.

(Managing Editor: WANG Caihong)